

Characterization of Oxoperoxo(2,6-pyridinedicarboxylato)molybdenum(VI) and Oxoperoxo(nitrilotriacetato)molybdate(VI) in Aqueous Solution and a Kinetic Study of Their Reduction by a (Thiolato)cobalt(III) Complex, Dimethyl Sulfoxide, and Iron(II)

Tae-Jin Won, Balakrishna M. Sudam, and Richard C. Thompson*

Department of Chemistry, University of Missouri—Columbia, Columbia, Missouri 65211

Received March 18, 1994*

Formation constants have been determined for the complexes $\text{MoO}(\text{O}-\text{O})(\text{dipic})$ and $\text{MoO}(\text{O}-\text{O})(\text{nta})^-$ at 25 °C with $I = 0.10 \text{ M}$ (NaCl). For the general formula $(\text{MoO}_4)(\text{L})(\text{H}^+)_4(\text{H}_2\text{O}_2)$, $\log K_f$ values of 23.48 and 23.0 were determined for $\text{L} = \text{dipic}$ by potentiometry and spectrophotometry, respectively; for $\text{L} = \text{nta}$, the corresponding $\log K_f$ values were 27.87 and 28.8. A single-crystal X-ray structure was determined for the nta complex, and ^{95}Mo NMR spectra were collected. The dipic complex is much more labile than the nta analogue. The rate of loss of peroxide from the complexes was measured by use of the peroxide "trapping agents" $\text{S}(\text{IV})$ and $\text{Zr}(\text{IV})$; first-order rate constants (s^{-1}) at 25 °C were, for dipic, 0.03 at pH 1 and, for nta, 1×10^{-4} at pH 1 and 5×10^{-6} at pH 4. Rate constants ($\text{M}^{-1} \text{ s}^{-1}$, at 25 °C) for the oxygen atom transfer reactions with $(\text{en})_2\text{Co}(\text{SCH}_2\text{CH}_2\text{NH}_2)_2^{2+}$ and $(\text{CH}_3)_2\text{SO}$ were, for $\text{MoO}(\text{O}-\text{O})(\text{dipic})$, 8.6×10^2 and 7.6×10^{-3} and, for $\text{MoO}(\text{O}-\text{O})(\text{nta})^-$, 2.5×10^3 and 5.8×10^{-3} , respectively. These reactivities are approximately the same as observed previously with the oxo diperoxo complex $\text{MoO}(\text{OH})(\text{O}-\text{O})_2^-$. Activation of coordinate peroxide was also observed in the kinetics of reduction by iron(II), with rate constants of 260 and $3.0 \times 10^3 \text{ M}^{-1} \text{ s}^{-1}$ at 25 °C for the dipic and nta oxo monoperoxo complexes, respectively. No intermediate was detected in either reaction, whereas one formulated as a superoxo complex is formed in the reduction of oxodiperoxo molybdates by iron(II).

Introduction

The early transition metals in their highest oxidation state rapidly react with hydrogen peroxide in aqueous solution to form robust peroxo complexes.^{1,2} The structure, formation constants, and kinetic parameters for a number of these d^0 complexes have been determined. The reactivity of the coordinated peroxo ligand(s), usually bonded in an η^2 fashion, as an oxygen atom transfer or one-electron oxidizing agent is enormously dependent on the metal ion center. To date, the oxo diperoxo complexes of Mo(VI) and W(VI) and $\text{CH}_3\text{ReO}_2(\text{O}-\text{O})$ are by far the most reactive.³⁻⁵ We previously found⁶ that the oxo monoperoxo complex $\text{VO}(\text{O}-\text{O})^+$ was much less reactive than $\text{VO}(\text{O}-\text{O})_2^-$. However, since V(V) at best only weakly activates coordinated peroxide, it would be of interest to compare the corresponding complexes of Mo(VI) (equilibrium measurements for peroxo complexes of W(VI) in acidic solution have not been reported, presumably due to the complex chemistry of free W(VI)). The experimental difficulty is the large stability of the oxo diperoxo species. Nevertheless, we have succeeded in stabilizing oxoperoxo molybdenum(VI) in aqueous solution through the use of the chelating agents 2,6-pyridinedicarboxylate (dipic) and nitrilotriacetate (nta) as heteroligands. We report in this article studies of their substitution kinetics and reactivity as oxygen atom transfer and one-electron oxidizing agents. The complexes have been characterized in solution by means of potentiometry, spectrophotometry, and ^{95}Mo NMR and in the solid state by single-crystal X-ray diffraction.

Experimental Section

Reagents. The preparation and standardization of solutions of Mo(VI), H_2O_2 , $\text{Fe}(\text{ClO}_4)_2$, and LiClO_4 have been described previously.^{7,8} H_2dipic , H_3nta , Na_2dipic , and Na_3nta (each of 99% purity) were obtained from Aldrich Chemical Co. The perchlorate salt of (2-aminoethanethiolato-*N,S*)bis(1,2-ethanediamine)cobalt(III) was prepared by the method of Nosco and Deutsch.⁹ Dimethyl sulfoxide was distilled under vacuum before use. All other chemicals were of reagent grade and were used as supplied. Deionized water was distilled twice before use; the last distillation was from alkaline permanganate.

Potentiometric Studies.^{10,11} An Orion semimicro Ross combination pH electrode attached to an Orion Research pH meter Model No. 601 was used. A double-walled glass vessel was employed for the titrations and maintained at 25.0 ± 0.1 °C. CO_2 was rigorously excluded by continuously bubbling N_2 through the reaction vessel and by the use of a guard tube for the aqueous NaOH titrant. All the formation constants determined were in concentration units. Therefore, the pH meter and the electrode system were calibrated in terms of $-\log [\text{H}^+]$ by titration of standardized HCl against standardized NaOH before each experiment. Ionic strength was maintained at 0.10 M by use of NaCl. Between 40 and 80 volume, pH data points were collected for each experiment. The data were analyzed by use of the computer program BEST.^{11,12}

Dilute solutions of Mo(VI) ($(1.00\text{--}2.00) \times 10^{-3} \text{ M}$) and excess complexing agent (dipic, nta, H_2O_2) were used to minimize the importance of polynuclear forms of Mo(VI). We found that no significant differences resulted if heptameric and octameric forms¹³ were included or omitted in the modeling; the reported values are those obtained by omitting polynuclear forms. The experimental conditions were designed to provide a significant variation in the concentration of the species of principal interest ($\text{MoO}_3(\text{dipic})_2^-$, $\text{MoO}_3(\text{nta})_3^-$, $\text{MoO}(\text{O}-\text{O})(\text{dipic})$, $\text{MoO}(\text{O}-\text{O})$ -

* Abstract published in *Advance ACS Abstracts*, July 15, 1994.

- (1) Connor, J. A.; Ebsworth, E. A. V. *Adv. Inorg. Chem. Radiochem.* **1964**, *6*, 279.
- (2) Mimoun, H. In *The Chemistry of Peroxides of Peroxides*; Patai, S., Ed.; Interscience: New York, 1983; pp 463-482.
- (3) Ghiron, A. F.; Thompson, R. C. *Inorg. Chem.* **1988**, *27*, 4766.
- (4) Schwane, L. M.; Thompson, R. C. *Inorg. Chem.* **1989**, *28*, 3938.
- (5) Huston, P.; Espenson, J. H.; Bakac, A. *Inorg. Chem.* **1993**, *32*, 4517.
- (6) Ghiron, A. F.; Thompson, R. C. *Inorg. Chem.* **1990**, *29*, 4457. The oxo monoperoxo and oxo diperoxo complexes we consider in this paper are pentagonal bipyramidal, with η^2 bound peroxo ligand(s) in the equatorial plane and an apical oxygen. The formulas given usually will not include coordinated water molecules.

- (7) Lydon, J. D.; Schwane, L. M.; Thompson, R. C. *Inorg. Chem.* **1987**, *26*, 2606.
- (8) Thompson, R. C. *Inorg. Chem.* **1986**, *25*, 184.
- (9) Nosco, D. L.; Deutsch, E. *Inorg. Synth.* **1982**, *21*, 859.
- (10) Sudam, B. M. M.S. Thesis, University of Missouri—Columbia, Columbia, MO, 1993. In general, the procedures used followed those recommended in ref 11.
- (11) Martell, A. E.; Motekaitis, R. J. *Determination and Use of Stability Constants*, 2nd ed.; VCH Publishers, Inc.: New York, 1992.
- (12) Motekaitis, R. J.; Martell, A. E. *Can. J. Chem.* **1982**, *60*, 2403.
- (13) (a) Yagasaki, A.; Andersson, I.; Pettersson, L. *Inorg. Chem.* **1987**, *26*, 3926. (b) Tytko, K. H.; Beathe, G.; Cruywagen, J. J. *Inorg. Chem.* **1985**, *24*, 3132.

Table 1. Crystal Data, Structure Determination, and Refinement Data for K[MoO(O-O)(nta)] · H₂O

formula	C ₆ H ₈ NO ₁₀ KMo
<i>M_r</i>	389.17
space group	<i>P</i> 2 ₁ / <i>n</i>
<i>a</i> (Å)	6.434(2)
<i>b</i> (Å)	11.062(3)
<i>c</i> (Å)	16.074(4)
β (deg)	100.56(2)
<i>V</i> (Å ³)	1124.7(5)
<i>Z</i>	4
<i>D_c</i> (g · cm ⁻³)	2.298
μ (cm ⁻¹)	15.5
<i>F</i> (000)	768
cryst size (mm)	0.05 × 0.08 × 0.35
radiation	Mo Kα
λ (Å) (graphite monochromator)	0.710 73
diffractometer	Enraf-Nonius CAD4
orienting reflns, range (deg)	25, 11 < θ < 15
temp (°C)	22 ± 1
scan method	ω-2θ
data collcn range	2.0 < 2θ < 46°
no. of data measd	1969
no. of unique data	1558
<i>R_i</i> (data averaging) (%)	2.1
no. of obsd data (<i>I</i> > 2.0σ(<i>I</i>), <i>N</i>)	1163
no. of params, <i>P</i>	172
<i>R^a</i> (%)	2.6
<i>R_w^b</i> (%)	3.5
<i>S</i> , goodness of fit ^c	0.90
max shift/error, final	<0.01
largest positive peak (e/Å ³)	0.43
largest negative hole (e/Å ³)	-0.40

^a $R = \sum(|F_o| - |F_c|) / \sum|F_o|$. ^b $R_w = \{\sum w(|F_o| - |F_c|)^2 / \sum w|F_o|^2\}^{1/2}$; $w = 1 / [(\sigma F_o)^2 + 0.001 F_o^2]$. ^c $S = \{\sum w(|F_o| - |F_c|)^2 / (N - P)\}^{1/2}$.

(nta)⁻ during the titration. The speciation diagrams revealed that the optimum pH values for forming these species were ca. 3.7, 3.9, 1.1, and 2.2. Starting the titrations of solutions containing H₂O₂ on the acid end has the advantage that little if any decomposition of peroxide is encountered until ca. pH 9–10, where nearly all the peroxide is uncomplexed. Light was excluded during titrations involving peroxide.

Synthesis and Crystal Structure of K[MoO(O-O)(nta)] · H₂O. The salt was prepared by addition of 1.9 g of H₃nta (10 mmol) to 12 mL (11 mmol) of 3% H₂O₂, followed by the addition of 2.4 g of K₂MoO₄ · 2H₂O (10 mmol). The pH was adjusted to ca. 2 by slow addition of 10 mL of 1 M HCl with stirring, and the resulting solution was diluted to 100 mL with water. This solution was cooled overnight at 0 °C and filtered. A 1.0-g amount of KNO₃ was slowly added to the filtrate with stirring, and the solution was cooled for 2–3 h at 0 °C. The bright yellow crystals were collected by filtration, washed with ethanol, and air dried. Yield: 0.8 g. Recrystallization of the solid from a mixture of ethanol and water gave yellow needle-shaped crystals, suitable for X-ray analysis. Elemental analysis (Galbraith Laboratories, Inc.) gave the following values [% found (% calcd)]: for Mo, 25.54 (24.65); for K, 10.56 (10.05); for H₂O, 5.83 (4.63). The solid does not detonate or show any signs of decomposition when struck with a hammer.

X-ray diffraction data were collected on an Enraf-Nonius CAD4 diffractometer using Mo Kα radiation (λ = 0.710 73 Å). The structure was solved by a combination of Patterson and direct methods and completed by successive Fourier calculations. The structure was refined by full-matrix least-squares methods, with anisotropic thermal parameters for all non-H atoms. The H atoms of the water molecule could not be located with confidence and were omitted from the final model, while those of the nta moiety were included at calculated positions with fixed isotropic thermal parameters. All calculations were performed with the NRCVAX program package.¹⁴ Details of the X-ray experiment, crystal data, data collection, reduction, and refinement are given in Table 1.

We were unsuccessful in efforts to obtain crystals of the putative [MoO(O-O)(Hnta)]. Solutions containing equimolar amounts of molybdate, hydrogen peroxide, and nta were adjusted to pH 1 by the slow addition of 1 M HCl and cooled overnight at 0 °C. An intractable oily mass resulted that was insoluble in organic solvents such as ethanol, acetone,

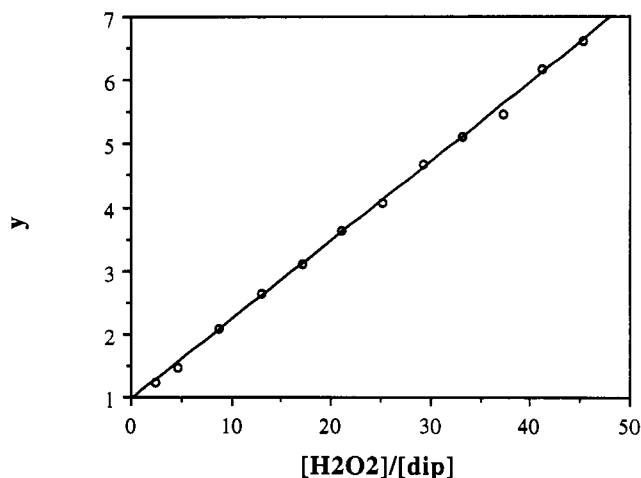
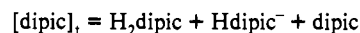
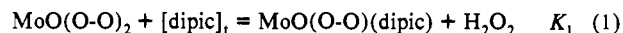


Figure 1. Plot for determination of equilibrium constant between oxidiperoxomolybdenum(VI) and oxoperoxo(2,6-pyridinedicarboxylato)-molybdenum(VI) at pH 1.0. $y = (\epsilon_{\text{MoO}(\text{O}-\text{O})_2(\text{dip})} - \epsilon_{\text{MoO}(\text{O}-\text{O})_2}) / (\epsilon_{\text{obs}} - \epsilon_{\text{MoO}(\text{O}-\text{O})_2})$. Conditions: $[\text{Mo}(\text{VI})]_0 = 1.0 \times 10^{-4} \text{ M}$; $[\text{dipic}]_0 = 5.0 \times 10^{-3} \text{ M}$; $[\text{H}_2\text{O}_2]_0 = 0.01\text{--}0.22 \text{ M}$; $T = 25 \text{ }^\circ\text{C}$.

benzene, chloroform, and acetonitrile. We were also frustrated in attempts to obtain crystals of, presumably, K₂[MoO₃(dipic)].

Spectrophotometric Titrations. Spectral changes occur in the near-UV region when dipic is added to solutions of MoO(O-O)₂. The absorption peak for the latter at 328 nm decreases, and a new peak at 364 nm due to MoO(O-O)(dipic) appears. An isobestic point is observed at 354 nm. Conditions were chosen for the equilibrium studies that (1) utilized dilute (≤ 1 mM) solutions of Mo(VI) to avoid the formation of polynuclear species and (2) maintained at least 99% of the Mo(VI) in the form of the two peroxo complexes. The equilibrium constant *K*₁ was determined by careful spectrophotometric titrations monitored at 400 nm, where the spectral difference between the two peroxo complexes is favorable, in 0.10 M HClO₄ and at 25.0 °C.

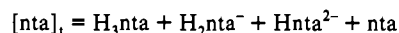
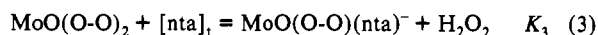


It can be shown that eq 2 should hold, where ϵ_{dip} (573 M⁻¹ cm⁻¹), $\epsilon_{2:1}$ (183

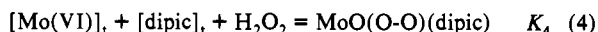
$$(\epsilon_{\text{dip}} - \epsilon_{2:1}) / (\epsilon_{\text{obs}} - \epsilon_{2:1}) = 1 + [\text{H}_2\text{O}_2] / \{K_1[\text{dipic}]\} \quad (2)$$

M⁻¹ cm⁻¹), and ϵ_{obs} are the extinction coefficients of MoO(O-O)(dipic), MoO(O-O)₂, and each reaction mixture, respectively. A value of *K*₁ = 7.8 was obtained from the linear plot shown in Figure 1.

A similar procedure was used to determine a value of *K*₃ = 4.6. The conditions were as follows: $[\text{Mo}(\text{VI})] = 5.00 \times 10^{-4} \text{ M}$; $[\text{H}_2\text{O}_2] = 2.5 \times 10^{-3} \text{ M}$, $[\text{nta}]_t = (0.75\text{--}6.00) \times 10^{-3} \text{ M}$; $[\text{HClO}_4] = 0.10 \text{ M}$; $T = 25.0 \text{ }^\circ\text{C}$; $\lambda = 400 \text{ nm}$ (where $\epsilon_{\text{nta}} = 499 \text{ M}^{-1} \text{ cm}^{-1}$).



We also determined the conditional formation constant *K*₄ by using hydrogen peroxide as the limiting reagent and thereby eliminating MoO(O-O)₂ as a significant species. The experimental conditions and results are summarized in Table S4; the average value of *K*₄ is 3.6 × 10⁸ in 0.10 M HClO₄ at 25 °C.



⁹⁵Mo NMR Studies. A Bruker AMX-500 NMR spectrometer operating at 32.5 MHz was used. The reported chemical shifts are relative to the external reference which was a 2 M Na₂MoO₄ solution containing 10% D₂O and adjusted to pH 11.0. Chemical shifts of 67 and 58 ppm

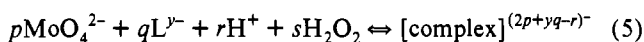
(14) Gabe, E. J.; Le Page, Y.; Charland, J.-P.; Lee, F. L.; White, P. S. *J. Appl. Crystallogr.* 1989, 22, 348–387.

were measured for $\text{MoO}_3(\text{nta})^{3-}$ and the species we formulate as $\text{MoO}_3(\text{dipic})^{2-}$, respectively.

Kinetic Studies. Either a Zeiss PMQII or a HP8452A diode array spectrophotometer, each equipped with a thermostated ($\pm 0.1^\circ\text{C}$), rapid-mixing (ca. 1 s) sample compartment, was used to monitor the slower reactions, and a Durrum D-110 stopped-flow instrument was used for the rapid reactions.

Results

Formation Constants and Spectra of $\text{MoO}(\text{O-O})(\text{dipic})$ and $\text{MoO}(\text{O-O})(\text{nta})^-$ in Aqueous Solution. The experimental conditions used in the potentiometric titrations were designed to facilitate the determination of the formation constants for the desired complexes (see Experimental Section). In particular, conditions were identified where only monomeric molybdenum(VI) species were of significance. All potentiometric data were collected at 25.0°C and $I = 0.10\text{ M}$, maintained by use of NaCl . The equilibria are represented by eq 5, and the overall formation



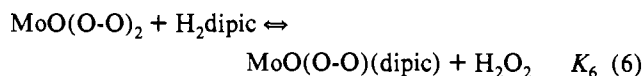
constants are referred to as β_{pqrs} . Values determined for the protonation constants for dipic ($\log \beta_{0110} = 4.71 \pm 0.02$ and $\log \beta_{0120} = 6.80 \pm 0.02$) and nta ($\log \beta_{0110} = 9.60 \pm 0.02$, $\log \beta_{0120} = 12.09 \pm 0.03$, and $\log \beta_{0130} = 13.86 \pm 0.02$) are in satisfactory agreement with those reported previously.¹⁵ Literature values for the protonation constants β_{1010} , β_{1020} , and β_{1030} of molybdate were used.^{16,17} Complexation of Mo(VI) by dipic was investigated with $2.00 \times 10^{-3}\text{ M Mo(VI)}$ and 6.00×10^{-3} , 8.00×10^{-3} , and $12.00 \times 10^{-3}\text{ M dipic}$. The potentiometric data were analyzed with the computer program BEST, and the model invoking only one complex, $[\text{1,1,2,0}]^{2-}$, along with the indicated protonation constants, adequately correlated the data ($\sigma_{\text{av}} = 0.030$) with $\log \beta_{1120} = 11.53 \pm 0.09$. The corresponding nta system was studied with $1.00 \times 10^{-3}\text{ M Mo(VI)}$ and $3.00 \times 10^{-3}\text{ M nta}$ and also with $5.00 \times 10^{-4}\text{ M Mo(VI)}$ and $1.5 \times 10^{-3}\text{ M nta}$. The calculations clearly showed the presence of the complex $[\text{1,1,2,0}]^{3-}$ and, in addition, but with less certainty, the complex $[\text{1,1,3,0}]^{2-}$ ($\sigma = 0.029$). Our values of $\log \beta_{1120} = 16.82 \pm 0.03$ and $\log \beta_{1130} = 19.2 \pm 0.2$ are not in very good agreement with those determined by Cruywagen et al.¹⁸ (17.78 and 21.02, respectively, at $I = 1.0\text{ M}$). However, this discrepancy is probably due to different experimental conditions, especially ionic strength, and to a certain extent the choice of models. We found that attainment of stable pH readings was quite slow in this system. The values of the formation constants for the peroxo complexes (see below) were not very sensitive to the values used for the Mo(VI) -heteroligand complexes.

Peroxo complexes of d^0 metal ions have only rarely been examined potentiometrically,¹⁹ but we found that reliable results could be obtained provided certain precautions were followed (see Experimental Section). In addition to the protonation constants (for dipic and MoO_4^{2-}) and the formation constant for the Mo(VI) -dipic complex, formation constants for $\text{MoO}(\text{O-O})_2(\text{H}_2\text{O})_2$ ($\log \beta_{1022} = 15.27$), $\text{MoO}(\text{OH})(\text{O-O})_2(\text{H}_2\text{O})^-$ ($\log \beta_{1012} = 13.41$), and $\text{MoO}_2(\text{O-O})_2^{2-}$ ($\log \beta_{1002} = 3.7$), taken from our previous work,^{7,20} and a pK_a value of 11.6 for H_2O_2 were included in the modeling. For the Mo(VI) -dipic- H_2O_2 system we used $2.00 \times 10^{-3}\text{ M Mo(VI)}$ with (a) $1.40 \times 10^{-2}\text{ M dipic}$ and $5.00 \times 10^{-3}\text{ M H}_2\text{O}_2$, and (b) $9.90 \times 10^{-3}\text{ M dipic}$ and $2.00 \times$

$10^{-3}\text{ M H}_2\text{O}_2$. The potentiometric data were satisfactorily correlated ($\sigma = 0.011$) by invoking only one quaternary complex, $[\text{1,1,4,1}]$, with $\log \beta_{1141} = 23.48 \pm 0.16$. Under the stated experimental conditions, the concentration of this complex was ca. 99% of the total Mo at the start of the titrations ($\text{pH} = 1.9$ – 2.0).

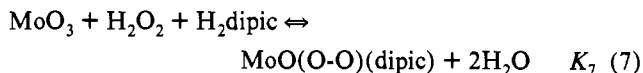
Initial concentrations used for the Mo(VI) -nta- H_2O_2 system were $1.00 \times 10^{-3}\text{ M Mo(VI)}$, $2.00 \times 10^{-2}\text{ M H}_2\text{O}_2$, and $(3.00$ – $5.00) \times 10^{-3}\text{ M nta}$. The calculations indicated two quaternary complexes, $[\text{1,1,4,1}]^-$ and $[\text{1,1,5,1}]$, with $\log \beta$ values of 27.87 ± 0.05 and 28.97 ± 0.25 . The concentration of the anionic species was as high as 69% at the optimum pH of 2.17. Evidence for the neutral complex comes only at low pH values, and its calculated concentration never exceeded 15% of the total Mo(VI) under our experimental conditions for the potentiometric titrations.²¹

We were able to measure the equilibrium constant K_6 in 0.10 M HClO_4 at 25°C by spectrophotometry.



The absorption spectra of $\text{MoO}(\text{O-O})_2$ (λ_{max} at 328 nm with $\epsilon = 1040\text{ M}^{-1}\text{ cm}^{-1}$) and $\text{MoO}(\text{O-O})(\text{dipic})$ ($\lambda_{\text{max}} = 364\text{ nm}$ with $\epsilon = 878\text{ M}^{-1}\text{ cm}^{-1}$) are sufficiently different to allow spectrophotometric titrations with differing $[\text{H}_2\text{dipic}]/[\text{H}_2\text{O}_2]$ ratios. Conditions were chosen such that $<1\%$ of the total Mo(VI) was present in forms other than the two peroxo complexes. The experimental conditions and data analysis are summarized in the Experimental Section; a value of 8.4 for K_6 was determined.

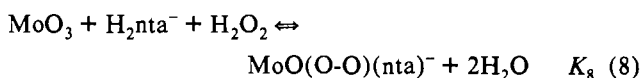
We also measured the equilibrium constant K_7 in 0.10 M HClO_4 at 25°C by using hydrogen peroxide as the limiting reagent, thereby effectively eliminating the formation of $\text{MoO}(\text{O-O})_2$ (under these conditions, the principal forms of uncomplexed Mo(VI) are MoO_3 and HMoO_3^+).



Again, the experimental conditions and data analysis are summarized in the Experimental Section; the value of K_7 was 8.3×10^8 . This is in excellent agreement with the value of 8.5×10^8 calculated from K_6 .

A value of $\log \beta_{1141} = 23.0$ for $\text{MoO}(\text{O-O})(\text{dipic})$ can be calculated from that determined spectrophotometrically for K_1 (see Experimental Section) by use of protonation constants (for dipic and MoO_4^{2-}) and formation constants (for $\text{MoO}(\text{O-O})_2$, $\text{MoO}(\text{OH})(\text{O-O})_2^-$, and $\text{MoO}_2(\text{O-O})_2^{2-}$). We consider the agreement between the potentiometric (23.5) and spectrophotometric results to be satisfactory.

The absorption spectra of $\text{MoO}(\text{O-O})(\text{nta})^-$ and $\text{MoO}(\text{O-O})(\text{dipic})$ are nearly identical. No spectral evidence for protonation of the former was found, even in molar perchloric acid. We determined a value of 3.6×10^9 for K_8 ; this leads to a value for $\log \beta_{1141} = 28.8$ for $\text{MoO}(\text{O-O})(\text{nta})^-$.



⁹⁵Mo NMR spectra, with chemical shifts reported relative to 2 M MoO_4^{2-} at pH 11.0 as external reference standard, were as follows: $\text{MoO}(\text{O-O})_2$, -193 ppm ; $\text{MoO}(\text{O-O})(\text{dipic})$, -128 ppm ; $\text{MoO}(\text{O-O})(\text{nta})^-$, -23 ppm . A solution containing equal concentrations of $\text{MoO}(\text{O-O})_2$ and $\text{MoO}(\text{O-O})(\text{dipic})$, based on the equilibrium results, showed the two predicted NMR peaks

(21) However, the data indicate that it should be the predominant nta peroxo complex in 0.10 M HClO_4 , a medium used for many of our kinetic studies.

(15) Martell, A. E.; Smith, R. M. *Critical Stability Constants*; Plenum Press, New York, 1989; Vol. 6, Second Supplement.

(16) Cruywagen, J. J.; Heyns, J. B. B. *J. Chem. Educ.* **1989**, *66*, 861.

(17) Cruywagen, J. J.; Heyns, J. B. B.; Rohwer, E. F. C. H. *J. Inorg. Nucl. Chem.* **1976**, *38*, 2033.

(18) Cruywagen, J. J.; Heyns, J. B. B.; Rohwer, E. A. *J. Chem. Soc., Dalton Trans.* **1994**, 45.

(19) Csanyii, L. *J. Acta Chim. Acad. Sci. Hung.* **1958**, *14*, 79.

(20) Islam, M. A.; Bray, D. G.; Bruecken, A. J.; Thompson, R. C. Unpublished work.

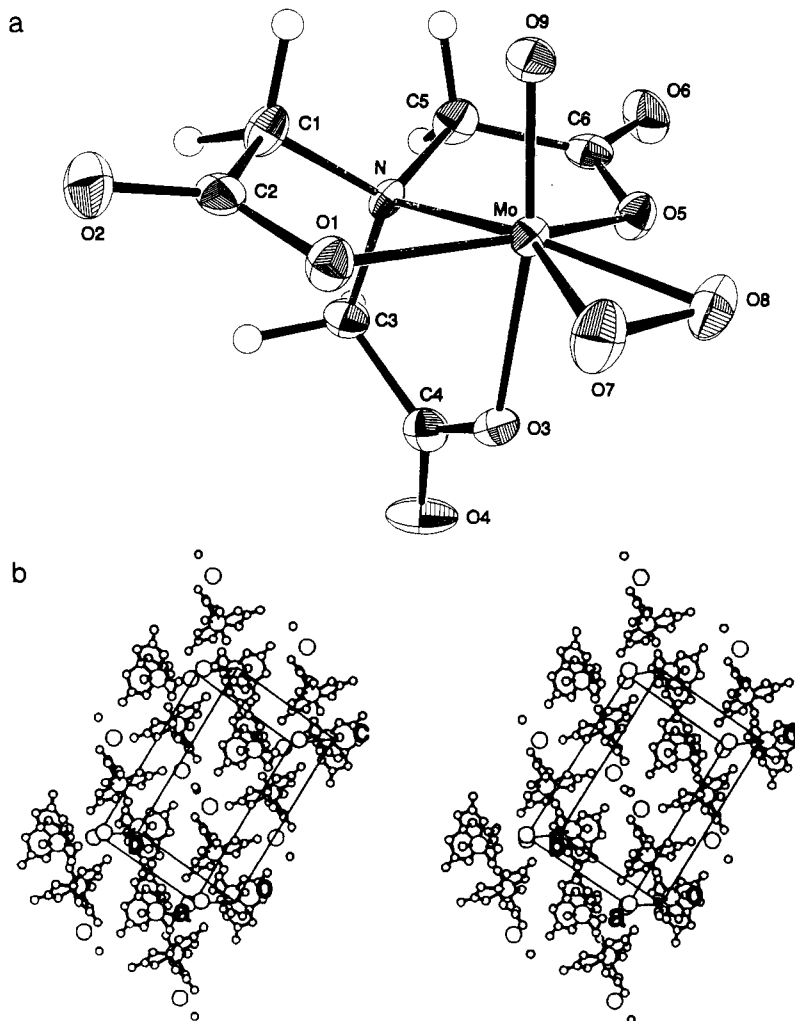


Figure 2. (a) Structure of the oxoperoxo(nitriilotriacetato)molybdenum(VI) ion in $\text{K}[\text{MoO}(\text{O}-\text{O})(\text{nta})] \cdot \text{H}_2\text{O}$. (b) Stereoview showing the crystal packing of $\text{K}[\text{MnO}(\text{O}-\text{O})(\text{nta})] \cdot \text{H}_2\text{O}$ in a unit cell.

with approximately equal integrated peak areas. No ^{95}Mo NMR evidence was obtained for a protonated nta peroxo complex; the same peak was observed from pH 1.0 to 4.0.

Single-Crystal X-ray Structure of $\text{K}[\text{MoO}(\text{O}-\text{O})(\text{nta})] \cdot \text{H}_2\text{O}$. The structure of the $\text{MoO}(\text{O}-\text{O})(\text{nta})^-$ anion and the crystal packing in the unit cell are shown in Figure 2. The geometry about the molybdenum is approximately pentagonal bipyramidal, with the equatorial plane occupied by the nitrogen and two carboxylate oxygen atoms of the heteroligand and the η^2 bonded peroxo group. The molybdenum atom is displaced 0.22 Å from the plane toward the oxo ligand. Full coordination of nta is completed by an elongated carboxylate oxygen—molybdenum bond in an apical position. The final atomic coordinates and selected bond distances and angles are listed in Tables 2 and 3, respectively. The peroxo O—O distance is within the range found for other oxoperoxomolybdates and is significantly shorter than that found in oxidiperoxomolybdates.²²

The previously reported structure for $[\text{MoO}(\text{O}-\text{O})(\text{dipic})] \cdot (\text{H}_2\text{O})$ is similar, with the apical positions occupied by the oxo oxygen and water molecule.²³

Kinetic Studies of the Formation and Decomposition of $\text{MoO}(\text{O}-\text{O})(\text{dipic})$ and $\text{MoO}(\text{O}-\text{O})(\text{nta})^-$. When a solution of Mo(VI) is rapidly mixed with one containing H_2O_2 and dipic at pH 1.0, the kinetic traces at 325 and 364 nm clearly indicate the rapid formation of $\text{MoO}(\text{O}-\text{O})_2$ followed by the much slower growth of $\text{MoO}(\text{O}-\text{O})(\text{dipic})$. The pseudo-first-order con-

Table 2. Atomic Parameters x , y , z , and B_{eq} , Where Esd's Refer to the Last Digit Printed

	x	y	z	B_{eq}^a (Å ²)
Mo	0.55516(7)	0.59323(4)	0.22584(3)	1.21(2)
N	0.2743(6)	0.4805(4)	0.1761(3)	1.2(2)
C1	0.3587(9)	0.3701(5)	0.1400(3)	1.8(2)
C2	0.5350(9)	0.4097(5)	0.0948(3)	1.7(2)
O1	0.6223(6)	0.5144(3)	0.1203(2)	1.8(2)
O2	0.5891(7)	0.3485(4)	0.0405(2)	2.7(2)
C3	0.1270(9)	0.5459(5)	0.1064(3)	1.8(2)
C4	0.1727(9)	0.6799(5)	0.1044(3)	1.8(2)
O3	0.3594(6)	0.7121(3)	0.1418(2)	1.6(2)
O4	0.0389(7)	0.7478(4)	0.0654(3)	2.8(2)
C5	0.1725(9)	0.4521(5)	0.2505(3)	1.9(2)
C6	0.2038(9)	0.5562(5)	0.3130(3)	1.7(2)
O5	0.3456(6)	0.6356(3)	0.3009(2)	1.9(2)
O6	0.1075(7)	0.5601(4)	0.3707(2)	2.7(2)
O7	0.7950(6)	0.6899(4)	0.2119(3)	2.4(2)
O8	0.6958(7)	0.7319(3)	0.2802(2)	2.5(2)
O9	0.6492(6)	0.4748(3)	0.2873(2)	2.0(2)
K	0.6403(2)	0.85466(12)	0.05558(8)	2.57(6)
OW	0.7695(8)	1.0862(4)	0.0333(3)	3.3(2)

^a B_{eq} is the mean of the principal axes of the thermal ellipsoid.

stant for the fast portion matches that previously reported for the formation of oxidiperoxomolybdenum(VI) under the same conditions except without dipic.⁷ No absorbance change is observed at the 354-nm isosbestic point for the two peroxo complexes when dipic is added to a solution of $\text{MoO}(\text{O}-\text{O})_2$ or H_2O_2 is added to a solution of $\text{MoO}(\text{O}-\text{O})(\text{dipic})$. We therefore studied the forward and reverse rates of eq 6 under conditions where >99% of the Mo(VI) was initially present as one or the

(22) Stomberg, R. *Acta Chem. Scand., Ser. A* 1988, A42, 284.

(23) Jacobson, S. E.; Tang, R.; Mares, F. *Inorg. Chem.* 1978, 17, 3055.

Table 3. Selected Bond Distances (Å) and Angles (deg) in $K[MoO(O-O)(nta)] \cdot H_2O$

Mo—N 2.220(4)	Mo—O1 2.024(3)	Mo—O3 2.126(4)
Mo—O5 2.022(4)	Mo—O7 1.924(4)	Mo—O8 1.910(4)
Mo—O9 1.685(4)	N—C1 1.496(6)	N—C3 1.513(7)
N—C5 1.498(6)	C1—C2 1.519(8)	C2—O1 1.319(7)
C2—O2 1.206(7)	C3—C4 1.513(8)	C4—O3 1.291(7)
C4—O4 1.224(7)	C5—C6 1.518(8)	C6—O5 1.307(7)
C6—O6 1.207(7)	O7—O8 1.444(6)	
N—Mo—O1 75.0(2)	N—Mo—O3 76.3(2)	N—Mo—O5 76.0(2)
N—Mo—O7 152.6(2)	N—Mo—O8 154.4(2)	N—Mo—O9 87.4(2)
O1—Mo—O3 85.80(14)	O1—Mo—O5 150.3(2)	O1—Mo—O7 81.0(2)
O1—Mo—O8 125.0(2)	O1—Mo—O9 92.7(2)	O3—Mo—O5 81.58(14)
O3—Mo—O7 88.7(2)	O3—Mo—O8 88.3(2)	O3—Mo—O9 164.0(2)
O5—Mo—O7 125.3(2)	O5—Mo—O8 81.5(2)	O5—Mo—O9 92.2(2)
O7—Mo—O8 44.3(2)	O7—Mo—O9 106.9(2)	O8—Mo—O9 105.5(2)
Mo—N—C1 105.6(3)	Mo—N—C3 110.9(3)	Mo—N—C5 106.1(3)
C1—N—C3 109.0(4)	C1—N—C5 112.4(4)	C3—N—C5 112.7(4)
N—C1—C2 107.8(4)	C1—C2—O1 114.7(4)	C1—C2—O2 121.6(5)
O1—C2—O2 123.7(5)	Mo—O1—C2 119.6(3)	N—C3—C4 112.7(4)
C3—C4—O3 115.4(5)	C3—C4—O4 119.4(5)	O3—C4—O4 125.2(5)
Mo—O3—C4 121.2(3)	N—C5—C6 110.2(4)	C5—C6—O5 115.0(5)
C5—C6—O6 120.8(5)	O5—C6—O6 124.2(5)	Mo—O5—C6 119.6(3)
Mo—O7—O8 67.3(2)	Mo—O8—O7 68.4(2)	

other peroxy complex. Representative kinetic data are presented in Table S5. In no case was the observed pseudo-first-order forward rate constant as large⁷ as that for dissociation of peroxide from $MoO(O-O)_2$. The reverse rate constant was linearly dependent on $[H_2O_2]$ over a substantial range.

We also examined eq 9, principally in the forward direction; the results are summarized in Table S6. The kinetic profiles



consisted of a rapid reaction (stopped-flow time scale) which appears to produce an intermediate, followed by a well-resolved slow reaction which forms $MoO(O-O)(nta)^-$. The kinetic traces for the reverse reaction were not biphasic and were very slow at pH 1.0. For example, a pseudo-first-order rate constant of $9.6 \times 10^{-5} s^{-1}$ was found with $[MoO(O-O)(nta)^-]_0 = 5.0 \times 10^{-4} M$, $[H_2O_2]_0 = 1.0 M$, $[HClO_4] = 0.10 M$, and $T = 25.0^\circ C$.

The decomposition of $MoO(O-O)(dipic)$ and $MoO(O-O)(nta)^-$ can be driven to completion by addition of a suitable hydrogen peroxide "trap". We used S(IV), which is rapidly oxidized by H_2O_2 under our experimental conditions but slowly by peroxomolybdates,^{7,24} and Zr(IV), which rapidly forms the peroxy complex²⁵ formulated as $Zr_4(O-O)_2(OH)_4^{8+}$. Plots of the pseudo first-order rate constant vs [trap] were linear (see Figure 3), with intercepts of $2.8 \times 10^{-2} s^{-1}$ and $3.2 \times 10^{-2} s^{-1}$ with S(IV) and Zr(IV), respectively, for the decomposition of $MoO(O-O)(dipic)$ at pH 1.0 and $25.0^\circ C$. More extensive studies were carried out with $MoO(O-O)(nta)^-$, since solutions prepared from the potassium salt were sufficiently stable in a kinetic sense to allow studies at pH values where the thermodynamic stability was negligible. The data are summarized in Table S7; intercepts (s^{-1}) from plots of k_{obs} vs [trap] were as follows: pH 1.0, 1.4×10^{-4} with S(IV) and 1.1×10^{-4} with Zr(IV); pH 4.0, 5.0×10^{-6} with S(IV) and 6.0×10^{-6} with Zr(IV). The data is strongly basic solution were consistent with the expression $k_{obs} = 3.0 \times 10^{-3} s^{-1} + 1.9 M^{-1} s^{-1} [OH^-]$.

Kinetic Studies of Oxygen Atom Transfer Reactions of $MoO(O-O)(dipic)$ and $MoO(O-O)(nta)^-$ and Their Reduction by Fe(II). The substitution-inert (thiolato)cobalt(III) complex $(en)_2Co(SCH_2CH_2NH_2)^{2+}$ has been a useful substrate for studying oxygen atom transfer reactions of peroxy complexes.^{3,5,6} The sulfenato product $(en)_2Co(S\{O\}CH_2CH_2NH_2)^{2+}$ is only very slowly further oxidized to the sulfinato complex. The reactions can be monitored sensitively by spectrophotometry. Since dilute solutions prepared

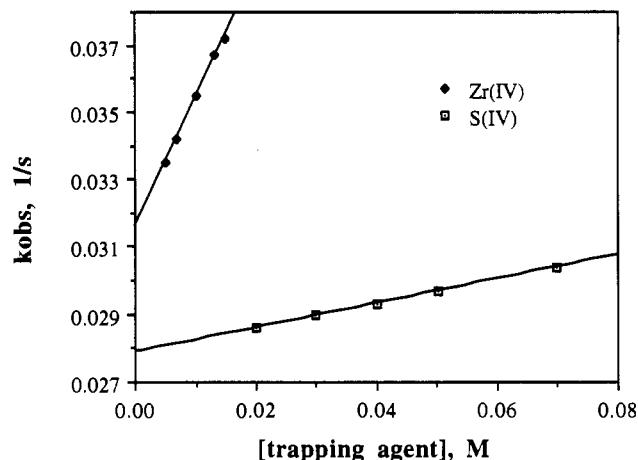


Figure 3. Graph to determine the rate constants for dissociation of oxoperoxo(2,6-pyridinedicarboxylato)molybdenum(VI) in the presence of the peroxide trapping agents Zr(IV) (diamonds) and S(IV) (squares) at pH 1.0. Conditions: $[Mo(VI)]_0 = 2.0 \times 10^{-4} M$; $[H_2O_2]_0 = 1.0 \times 10^{-3} M$; $[dipic] = 5.0 \times 10^{-3} M$; $T = 25^\circ C$.

Table 4. Kinetic Results for the Oxidation of Dimethyl Sulfoxide by Oxoperoxo(2,6-pyridinedicarboxylato)molybdenum(VI) and by Oxoperoxo(nitrilotriacetato)molybdenum(VI)^a

Mo(VI) complex	pH ^b	[DMSO] ₀ , M	$10^3 k_{obs}$, ^c s ⁻¹	$10^3 k_{2nd}$, ^d M ⁻¹ s ⁻¹
dipic	1.00	0.70	5.3	7.6
dipic	1.00	0.60	3.6	7.6
dipic	1.00	0.40	3.0	7.5
dipic	1.00	0.20	1.6	7.8
nta	1.00	0.60	3.4	5.7
nta	1.00	0.40	2.3	5.8
nta	1.00	0.20	1.2	5.7
nta	4.00	0.60	3.4	5.7
nta	4.00	0.40	2.2	5.8
nta	4.00	0.20	1.3	6.3

^a Monitored at 364 nm. $T = 25^\circ C$. For dipic studies, $[H_2O_2]_0 = 3.00 \times 10^{-4} M$, $[dipic]_0 = 4.0 \times 10^{-3} M$, and $[Mo(VI)] = (3.00-4.00) \times 10^{-4} M$. Solid $K[MoO(O-O)(nta)]$ used for nta studies. ^b 0.10 M $HClO_4$ used for pH 1.00, and 0.050 M acetate buffer ($I = 0.10 M$ by use of $LiClO_4$) used for pH 4.00. ^c Values listed are slopes of plots of $-\ln [A_\infty - A_t]$ vs t . ^d Values refer to rate law: rate = $k_{2nd}[Mo(VI) \text{ complex}][DMSO]$.

from solids containing $MoO(O-O)(dipic)$ are not stable with respect to at least partial dissociation, we formed the complex in solutions containing appropriate amounts of Mo(VI), dipic, and H_2O_2 . A large excess of the complex was used in the kinetic studies so problems with regeneration of the oxidant during the reaction could be avoided. The kinetic results and experimental conditions are summarized in Table S8. The rate expression is first order each with respect to $[MoO(O-O)(dipic)]$ and $[(thiolato)cobalt(III)]$. Only a small variation in the rate parameter with $[H^+]$ is observed over the range 0.010–1.0 M.

The corresponding results for $MoO(O-O)(nta)^-$ are collected in Table S9. Values of the second-order rate constant are the same ($2.5 \times 10^3 M^{-1} s^{-1}$) at pH 1.0 and 4.0 and are approximately thrice that for the dipic complex. With the neutral substrate dimethyl sulfoxide the rate difference between the two monoperoxy complexes is much smaller, as can be gleaned from the data compiled in Table 4.

The kinetics of the rapid oxidation of Fe^{2+} by oxodiperoxo-molybdates have been reported previously.⁴ An intermediate, proposed to be a reactive superoxomolybdenum(VI) complex, was detected. We examined the $Fe^{2+}-MoO(O-O)(dipic)$ reaction by monitoring the formation of Fe(III) at 300 nm by use of the stopped-flow instrument. No evidence for an intermediate was detected, and plots of $-\ln [A_\infty - A_t]$ vs t were linear. The rate expression given in eq 10 was determined under the following pseudo-first-order conditions: $[Mo(VI)] = 4.0 \times 10^{-5} M$; $[H_2O_2]_0$

(24) McArdle, J. V.; Hoffman, M. R. *J. Phys. Chem.* **1983**, *87*, 5425.

(25) Thompson, R. C. *Inorg. Chem.* **1985**, *24*, 3542.

Table 5. Percent MoO(O-O)(dipic) and MoO(O-O)(nta)⁻ Present at Equilibrium in Aqueous Solutions Prepared from Their Coordination Compounds as a Function of Concentration and pH at 25 °C^a

[MoO(O-O)(dipic)] ₀ , M	equilibrium percentage at pH =			
	1.0	2.0	3.0	4.0
1.0 × 10 ⁻⁴	83	75	22	0.4
1.0 × 10 ⁻³	94	85	36	1.8
1.0 × 10 ⁻²	94	85	37	3.8

[MoO(O-O)(nta) ⁻] ₀ , M	equilibrium percentage at pH =			
	1.0 ^b	2.0 ^b	3.0	4.0
1.0 × 10 ⁻⁴	17 (33)	49 (9)	16	0.3
1.0 × 10 ⁻³	27 (51)	63 (11)	31	1.2
1.0 × 10 ⁻²	27 (52)	63 (12)	32	2.6

^a Calculations take into account all species considered in the potentiometric studies and assume that no pH changes occur during dissociation of the oxo monoperoxo complexes. ^b Values in parentheses refer to MoO(O-O)(Hnta).

= 3.0 × 10⁻⁵ M, [dipic] = 4.0 × 10⁻⁴ M; [HClO₄] = 0.20 M; [Fe²⁺]₀ = (0.30–1.5) × 10⁻³ M; T = 25.0 °C.

$$-d[\text{MoO(O-O)(dipic)}]/dt = 260 \text{ M}^{-1} \text{ s}^{-1} [\text{MoO(O-O)(dipic)}][\text{Fe}^{2+}] \quad (10)$$

The kinetic traces for the corresponding MoO(O-O)(nta)⁻ system were biphasic, with a rapid increase in absorbance at 300 nm followed by a much slower one. The slow portion was identified as a substitution reaction of nta released in the rapid redox reaction with the Fe(III) also produced. This subsequent reaction was effectively eliminated by the presence of Zr(IV), which forms a nonabsorbing complex with nta very rapidly.²⁶ The kinetic results obtained with Zr(IV) as a nta scavenger are summarized in Table S10. The data are consistent with the rate expression given in eq 11, under the conditions [MoO(O-O)(nta)⁻]₀ = 1.00 × 10⁻⁴ M, [HClO₄] = 0.010–0.10 M with I = 0.10 M, [Fe²⁺]₀ = (1.0–2.5) × 10⁻³ M, and T = 25.0 °C.

$$-d[\text{MoO(O-O)(nta)}^-]/dt = 3.0 \times 10^3 \text{ M}^{-1} \text{ s}^{-1} [\text{MoO(O-O)(nta)}^-][\text{Fe}^{2+}] \quad (11)$$

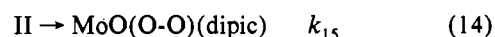
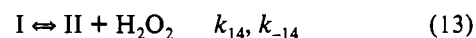
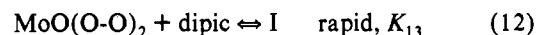
Discussion

The formation constants determined for MoO(O-O)(dipic) and MoO(O-O)(nta)⁻ appear to be reliable, particularly given the reasonable agreement between the potentiometric and spectrophotometric values. An interesting application is to assess the thermodynamic stability of aqueous solutions prepared from solid forms of the complexes. Some typical results are listed in Table 5, under the assumption that the pH values listed do not change as the complex dissociates. The results demonstrate that in addition to the formation constants for the complexes, which are very large in the present case, the concentration and especially the prevailing pH dictate the equilibrium concentrations. The kinetic data indicate, as do direct experiments, that equilibrium will be established rapidly with MoO(O-O)(dipic) and much more slowly with MoO(O-O)(nta)⁻.

The key to stabilizing oxoperoxomolybdenum(VI) complexes is to incorporate a heteroligand that can effectively coordinate three sites in the pentagonal plane. Bidentate ligands do not appear to be effective; instead, oxodiperoxomolybdates are usually formed with the heteroligand coordinated in one equatorial and (weakly) in one apical site.^{27,28} The values of the conditional constants K₁ and K₃ illustrate that even dipic and nta are only marginally stronger chelators of oxoperoxomolybdates than is

peroxide, although the comparison is somewhat marred by the feature that one and two water molecules, respectively, are also displaced in forming the heteroligand peroxo complex.

We examined the rates of formation of the heteroligand peroxo complexes principally at pH 1, where the thermodynamic stabilities are very large. What is observed first is the formation of oxodiperoxomolybdenum(VI), a kinetically controlled process that is probably due in part to the thermodynamic instability of MoO₃(nta)³⁻ and MoO₃(dipic)²⁻ at pH 1. We therefore studied in some detail the interconversions of the oxo diperoxo and the oxo monoperoxo complexes, processes that at least have pragmatic importance. Two notable differences in the formation of the heteroligand complexes are (1) an intermediate is observed in the nta system and (2) the dipic complex is formed much more rapidly. The following scheme is qualitatively in accord with the experimental data:



We suggest that the intermediate I is oxodiperoxo(dipic)-molybdenum(VI) and that its absorption spectrum is indistinguishable from that of MoO(O-O)₂. We at least have the precedent that the spectrum of MoO(O-O)₂(C₂O₄)²⁻ is virtually identical to that of MoO(O-O)₂ in the near UV.²⁸ In addition, the spectra of MoO(O-O)(dipic) and MoO(O-O)(nta)⁻ are nearly superimposable. Substitution is limited by peroxide loss from the intermediate I and is therefore never greater than the rate of peroxide loss from oxodiperoxomolybdenum(VI). The resulting intermediate II then closes to form product or reversibly gains peroxide again. This scheme also qualitatively predicts the observed [H₂O₂] and [dipic] dependencies, but we were unable to extend the concentration range sufficiently to test the scheme more quantitatively. Microscopic reversibility of course applies to the conversion of MoO(O-O)(dipic) to MoO(O-O)₂, but in addition we detect a pathway first order in [H₂O₂] that would not be seen in the reverse reaction, since the monoperoxo complex would be thermodynamically unfavored at such high concentrations of hydrogen peroxide. There is a labile, apical water molecule in MoO(O-O)(dipic) which could be displaced by peroxide.

This scheme is by no means unique, and we have difficulty in adapting it to the nta system. Here an intermediate is seen spectrally; it is not clear why it is observable here but not in the dipic reaction. It also is not clear why the final ligand closure to form MoO(O-O)(nta)⁻ is so slow, but it should be remembered that nta is tetradentate in the peroxo complex.

The decomposition studies of the monoperoxo complexes in the presence of trapping agents appear to allow a direct measure of the intrinsic rate of loss of peroxo ligand. This loss is relatively rapid in MoO(O-O)(dipic) (k = 0.03 s⁻¹) but much slower in MoO(O-O)(nta)⁻ (10⁻⁴ s⁻¹) at pH 1. For comparison, the rate constant is 0.2 s⁻¹ for MoO(O-O)₂ under the same conditions. Interestingly, the rate for the nta complex is not affected by the presence of molar hydrogen peroxide. Dissociation is promoted by hydroxide ion, but the kinetic stability of MoO(O-O)(nta)⁻ at pH 13 equals that of MoO(O-O)(dipic) at pH 1. The complex VO(O-O)(nta)²⁻ is also extraordinarily stable toward dissociation²⁹ and may prove useful in potential medical applications.³⁰

The three peroxo complexes MoO(O-O)₂, MoO(O-O)(dipic), and MoO(O-O)(nta)⁻ can be observed separately or in the presence of one another by ⁹⁵Mo NMR. These observations serve

(26) Intorre, B. J.; Martell, A. E. *Inorg. Chem.* **1964**, *3*, 81.

(27) Stomberg, R. J. *Crystallogr. Spectrosc. Res.* **1988**, *18*, 659.

(28) Ghiron, A. F.; Thompson, R. C. *Inorg. Chem.* **1989**, *28*, 3647.

(29) Sivak, M.; Joniakova, D.; Schwendt, P. *Transition Met. Chem.* **1993**, *18*, 304.

(30) Posner, B. I.; Faure, R.; Burgess, J. W.; Bevan, A. P.; Lachance, D.; Zhang-Sun, G.; Fantus, I. G.; Ng, J. B.; Hall, D. A.; Lum, B. S.; Shaver, A. J. *Biol. Chem.* **1994**, *269*, 4596.

to verify the equilibrium and kinetic results, respectively. The negative chemical shifts are characteristic of peroxomolybdates,³¹ in contrast to the positive values observed for MoO₃(nta)³⁻ and MoO₃(dipic)²⁻.³²⁻³⁴ We are reasonably confident of our formulation for the latter complex, but it is unclear what its structure is—the trioxo unit on molybdenum(VI) is invariably facial, but the orientation of the relatively rigid dipic ligand is not known.

Previous studies of the oxygen atom transfer reactions of oxodiperoxomolybdates in aqueous media have demonstrated that (1) the peroxo ligands are enormously activated relative to hydrogen peroxide and several other d⁰ metal analogues, (2) the oxygen atom transferred originates in the peroxo ligand, and (3) direct attack of the substrate at the peroxo ligand occurs, without prior coordination to the metal center.^{3,4,28} We presume that the latter two features obtain for the oxo monoperoxo complexes, and our interest here lies in the degree of activation of the peroxo ligand. Some relevant data have been assembled in Table 6. It is rather clear that the activation of the peroxo ligand in the two oxo monoperoxo complexes is close to that found in the hydrolyzed diperoxo complex MoO(OH)(O-O)₂⁻, at least for the two substrates tested. This conclusion is independent of whether the oxygen atom transfer reaction is relatively rapid, as with the (thiolato)cobalt(III) complex, or slow, as is the case with DMSO.

No intermediate is detected in the oxidation of iron(II) by either oxo monoperoxo complex, yet an intermediate formulated as a superoxo complex is formed with oxodiperoxomolybdates.⁴ We suggested previously that in the diperoxo reactions a hydroxyl radical, formed by the one-electron reduction of a peroxo ligand by iron(II), either oxidized the remaining peroxo ligand to superoxide or escaped the cage and rapidly oxidized another iron(II). The necessary second peroxo ligand is of course absent in the oxo monoperoxo complexes. Some relevant second order rate constants (M⁻¹ s⁻¹), at 25 °C, for the oxidation of iron(II) are

- (31) Dengel, A. C.; Griffith, W. P.; Powell, R. D.; Skapski, A. C. *J. Chem. Soc., Dalton Trans.* **1987**, 991.
 (32) Our measured chemical shift for the Mo(VI)-nta complex is in good agreement with the value given in ref 33. No value has been reported, to our knowledge, for the Mo(VI)-dipic complex. For an excellent discussion of the advantages of multinuclear NMR for Mo(VI) complexes, see ref 34.
 (33) Freeman, M. A.; Schultz, F. A.; Reilley, C. N. *Inorg. Chem.* **1982**, *21*, 567.
 (34) Castro, M. M. C. A.; Geraldes, C. F. G. C.; Peters, J. A. *Inorg. Chim. Acta* **1993**, *208*, 123.
 (35) Adzamlı, I. K.; Libson, K.; Deutsch, E.; Elder, R. C. *Inorg. Chem.* **1979**, *18*, 303.
 (36) Adzamlı, I. K.; Deutsch, E.; *Inorg. Chem.* **1980**, *19*, 1366.
 (37) Deutsch, E.; Root, M.; Nosco, D. L. In *Adv. Inorg. Bioinorg. Mech.* **1982**, *1*, 269.
 (38) Monzyk, M. M. M.S. Thesis, University of Missouri—Columbia, Columbia, MO, 1988.

Table 6. Summary of Rate Constants for the Oxidation of (Thiolato)cobalt(III) and Dimethyl Sulfoxide by Selected Oxoperoxomolybdates at 25 °C^a

substrate	oxidant	$k, {}^b \text{M}^{-1} \text{s}^{-1}$	ref
thiolato	MoO(O-O) ₂	1.9×10^4	3
thiolato	MoO(OH)(O-O) ₂ ⁻	2.4×10^3	3
thiolato	MoO(O-O)(dipic)	8.6×10^2	this work
thiolato	MoO(O-O)(nta) ⁻	2.5×10^3	this work
thiolato	H ₂ O ₂	1.4	35-37
DMSO	MoO(O-O) ₂	3.1×10^{-2}	38
DMSO	MoO(OH)(O-O) ₂ ⁻	2.4×10^{-3}	38
DMSO	MoO(O-O)(dipic)	7.6×10^{-3}	this work
DMSO	MoO(O-O)(nta) ⁻	5.8×10^{-3}	this work
DMSO	H ₂ O ₂	$\leq 5 \times 10^{-6}$	38

^a Ionic strength 0.10 M (by use of LiClO₄) except for MoO(O-O)₂ and H₂O₂-DMSO systems where it was 1.0. ^b Rate constants are for the general rate law: $R = k[\text{substrate}][\text{Mo(VI) complex or H}_2\text{O}_2]$.

as follows: MoO(OH)(O-O)₂⁻, 5.6×10^4 ; MoO(O-O)₂, 2.8×10^4 ; MoO(O-O)(nta)⁻, 3.0×10^3 ; MoO(O-O)(dipic), 2.6×10^2 ; H₂O₂, 63. We conclude that activation occurs in the monoperoxo complexes, albeit only weakly with dipic as the heteroligand. It is very likely that all of these reactions are inner sphere and, therefore, can be usefully compared with the oxygen atom transfer reactions.

The reactivity of peroxo ligands in d⁰ transition metal ion complexes is enormously variable. The reasons for this variation have been considered by a number of investigators; most treatments have focused on ground-state properties. Correlations based on O-O peroxo bond distances or stretching frequencies have met with limited success, at least in aqueous solution.^{6,39,40} High level, ab initio calculations on simple peroxomolybdates should be feasible in the near future.⁴¹ The results may reveal that transition-state properties are at least as important as those in the ground state.

Acknowledgment. This research was supported by the U.S. Army Research Office. We thank Charles Barnes for the single-crystal X-ray structure and acknowledge support of the NSF for the X-ray facility through Grant CHE 9011804.

Supplementary Material Available: Hydrogen atom coordinates and thermal parameters, anisotropic thermal parameters, and bond distances and angles (Tables S1-S3), formation constant data for MoO(O-O)(dipic) (Table S4), and kinetic data (Tables S5-S10) (10 pages). Ordering information is given on any current masthead page.

(39) Vaska, L. *Acc. Chem. Res.* **1976**, *9*, 175.

(40) Bonchio, M.; Conte, V.; Di Furia, F.; Modena, G.; Moro, S. *Inorg. Chem.* **1993**, *32*, 5797.

(41) Frenking, G. Marburg, Philipps Universitaet, private communication.